International Journal of Sciences: Basic and Applied Research (IJSBAR)

ISSN 2307-4531
(Print & Online)

http://gssrr.org/index.php?journal=JournalOfBasicAndApplied

Fast Fuzzy C-Means Algorithm Incorporating Convex Combination of Bilateral Filter with Contrast Limited Adaptive Histogram Equalization

K. Kadambavanam[a], T. Senthilnathan[b*]

[a]*Associate Professor and Head (Retd.), Department of Mathematics, Sri. Vasavi College, Erode, Tamil Nadu, India.*

[b]*Associate Professor, Department of Mathematics, Erode Arts and Science College, Erode-638 009, Tamil Nadu, India.*

[a]*Email: drkkvanam@yahoo.co.in*

[b]*Email: tstsenthilnathan@gmail.com*

Abstract

Fast Generalized Fuzzy c-means clustering algorithm (FGFCM) and its variants are effective methods for image clustering. Even though the incorporation of local spatial information to the objective function reduces their sensitivity to noise to some extent, they are still lack behind in suppressing the effect of noise and outliers on the edges and tiny areas of input image. This article proposes an algorithm to mitigate the disadvantage of FGFCM and its variants and enhances the performance of clustering. The experiments on the synthetic and real images are presented, to exhibit the improvements in the image clustering due to the proposed algorithm.

Keywords: Fuzzy logic; Image filtering; Histogram equalization; Impulse noise; Noise detection.

---

* Corresponding author.

1. Introduction

Clustering is the process of classifying data elements into divisions or clusters, so that data in the same cluster are as similar as possible. Image clustering has a spectrum of applications, such as, medical image segmentation [1, 2, 3, 4], remote sensing [5], and object recognition [6]. Fuzzy c-mean (FCM) [7] methods is very often used for image clustering [8, 9, 10, 4].

It is able to retain more information from the original image, than the hard clustering methods [11]. But it is very sensitive to noise. The reason for this is, in FCM, no spatial information in image context is taken into account.

Various researcher works have been done by imposing local spatial information into the standard FCM algorithm to promote the robustness of image clustering [12, 11, 13, 14]. By incorporating spatial constrains a Sugeno-model rule based system was developed by [14]. By introducing spatial penalty on membership functions, the FCM objective function was modified by Pham [15]. Further the objective function of FCM was modified in [16, 17]. These articles have proposed a new variance of FCM, called FCM_S, in which the intensity-inhomogeneity is reduced by labeling a pixel, which itself by the influence of the labels of its immediate neighborhood pixels [16]. The disadvantage in FCM_S is that it is a time-consuming one, as it calculates the neighborhood term in each iteration step. To reduce the computational time of FCM_S, Chen and Zhang have replaced the neighborhood term of the objective function of FCM_S with the mean filtered image (in FCM_S_1) / median filtered image (in FCM_S_2) in [18].

To accelerate the process of image clustering, in [19] enhanced fuzzy c-means (EnFCM) algorithm was proposed. Here the point taken into account in EnFCM is that, in general the number of gray scales q is very smaller than the total number of pixels N in an input image. By utilizing this fact, the process time of EnFCM can be reduced from $O(NcI_1)$ to $O(qcI_2)$, where $I1$ and $I2$ ($<I1$, generally) are the numbers of iterations in the standard FCM and EnFCM method respectively. The outline of EnFCM is different from, that of FCM_S and its variants. Initially, an image with linear-weighted sum of both mean filter image and the original image is created. Then, the resultant image is segmented on the basis of the gray values histogram instead of individual pixels in the image.

Even though, the computation time of EnFCM is reduced, the objective function of EnFCM still has a parameter α as in FCM_S and its variants. The parameter α is manually adjustable to make a balance between the original image and its corresponding mean/median-filtered image. Setting the value of α plays a vital role in the performance of these clustering methods. As α has to maintain a balance between effectiveness of preserving the details and insensitiveness to noise, in general, determining its value is tedious. In other words, assigning a value to α is depending on the noise in the input image to some extent. As the intensity and types of the noise, are generally unknown in advance, assigning the value of α has to be done by trial-and-error method or by experience [17, 18, 19]. In addition to that, the value of α is kept unchanged for all neighbor windows over the image. Thus the spatial information (or local gray level) of the image may be overlooked.

To overcome the above said defect (of assigning a value to α) and at the same time to improve the performance of image clustering, fast generalized fuzzy c-means algorithms (FGFCM) frame work has been introduced by [20]. In FGFCM, a modified bilateral denoising filter with an automated Gaussian distance weight S_{ij} was introduced to replace the parameter α.

But, when edge pixels and tiny areas in the input image are corrupted, bilateral filter is not performing well in denoising processes. To improve the FGFCM frame work further, this article proposes a contrast limited adaptive histogram equalization fast fuzzy c-means (AHFFCM) algorithm.

Experimental results on synthetic, real images establish that the proposed algorithm performs significantly better than the existing clustering algorithms. The rest of this article is organized into six sections as follows: In section 2**,** an introduction to fuzzy c-means clustering algorithms with spatial constraints (FCM_S, FCM_S_1 and FCM_S_2) are presented. EnFCM, FGFCM, FGFCM_S_1 and FGFCM_S_2 are briefed in section 3. An introduction to contrast limited local adaptive histogram equalization (CLAHE) and the proposed algorithm is presented in section 4. The experimental results are compared with the existing algorithms in section 5. Conclusions of this analysis, scope, and limitations of this proposed contrast limited AHFFCM algorithm are presented in section 6.

2. Preliminaries

2.1 Fuzzy c-Means clustering with spatial features (FCM_S)

In the standard FCM algorithm a modification was proposed by [16, 17]. The influence of neighboring pixels in labeling a pixel was considered in these articles. This makes a piecewise-homogeneity in labeling. The objective function of FCM_S is modified as

$$J_m = \sum_{i=1}^{C}\sum_{j=1}^{N} u_{ij}^{m} \| x_j - v_i \|^2 + \frac{\alpha}{|N_j|} \sum_{i=1}^{C}\sum_{j=1}^{N} u_{ij}^{m} \sum_{x_r \in N_j} \| x_r - v_i \|^2 \quad (1)$$

where $x_j \in \Re^P$ is the data set, $X = \{x_1, x_2, \ldots x_N\}$, u_{ij} - the degree to which element x_j belongs to the cluster i, $u_{ij} \in [0,1]$, $i = 1, 2, \ldots C$, $j = 1, 2, \ldots N$, $v_i \in \Re^P$ and $V = \{v_1, v_2, \ldots, v_c\}$ - prototype or centroids of the cluster i, N - number of data, C - number of clusters ($2 \leq C \leq N$), α - the controlling parameter of the neighbourhood feature, $|N_j|$- the cardinality of the neighbourhood feature, N_j - the set of neighbours of x_j,

x_r - the neighbouring data point around x_j falling in the window, with centre x_j , and m - a weighting exponent that determines the amount of fuzziness of the resulting classification.

The coefficient u_{ij} of x_j satisfies the condition that $\sum_{i=1}^{C} u_{ij} = 1$. Taking the first derivatives of J_m with respect to u_{ij} and v_i and equating them to zero, respectively, two necessary conditions for J_m are obtained as follows:

$$u_{ij} = \frac{\left[\| x_j - v_i \|^2 + \frac{\alpha}{|N_j|} \Sigma \| x_r - v_i \|^2 \right]^{\frac{-1}{(m-1)}}}{\sum_{k=1}^{C} \left[\|x_j - v_k\|^2 + \frac{\alpha}{|N_j|} \Sigma \|x_r - v_k\|^2 \right]^{\frac{-1}{(m-1)}}} \quad , \tag{2}$$

$$\text{and} \qquad v_i = \frac{\sum_{j=1}^{N} u_{ij}^m \left[x_j + \frac{\alpha}{|N_j|} \Sigma x_r \right]}{(1+\alpha) \sum_{j=1}^{N} u_{ij}^m} \tag{3}$$

where the summation of x_r runs over N_j. The quantity, $\frac{1}{|N_j|}\sum x_r$ in the equation (3) is the mean filter image. FCM_S takes much time for computation and is sensitive to noise in the input image.

2.2 Variants in FCM_S

To reduce the processing time of FCM_S, the set of neighbourhood pixels was replaced by its mean | median in the equations (1) - (3). In [18], the objective function is modified as

$$J_m = \sum_{i=1}^{C} \sum_{j=1}^{N} u_{ij}^m \| x_j - v_i \|^2 + \alpha \sum_{i=1}^{C} \sum_{j=1}^{N} u_{ij}^m \| \bar{x}_j - v_i \|^2 \tag{4}$$

where $\bar{x}_j$ represents the mean in FCM_S_1 or median in FCM_S_2.

The corresponding equations for u_{ij} and v_i are obtained as follows

$$u_{ij} = \frac{\left[\| x_j - v_i \|^2 + \alpha \| \bar{x}_j - v_i \|^2 \right]^{\frac{-1}{(m-1)}}}{\sum_{k=1}^{C} \left[\|x_j - v_k\|^2 + \alpha \|\bar{x}_j - v_k\|^2 \right]^{\frac{-1}{(m-1)}}}, \tag{5}$$

$$\text{and} \qquad v_i = \frac{\sum_{j=1}^{N} u_{ij}^m [x_j + \alpha \bar{x}_j]}{(1+\alpha) \sum_{j=1}^{N} u_{ij}^m}, \tag{6}$$

where $\bar{x}_j$ – the mean of the pixels in the local window in FCM_S_1 or median of the pixels in the local window in FCM_S_2.

To guarantee the gray homogeneity, the concept of FCM_S_1 is, to make both the original noiseless image and the corresponding mean-filter image get the same clustering result. But, FCM_S_1 is not suitable for the images corrupted by salt and pepper noise [18]. This problem is overcome by FCM_S_2 algorithm, by using the median-filter image instead of the mean-filter image.

3. Fast Fuzzy c-means clustering algorithms

3.1 Enhanced Fuzzy c-means clustering (EnFCM)

In order to reduce the clustering process-time for gray scale images, EnFCM algorithm is proposed by [19]. To

speed up, the clustering, a linearly-weighted sum image ξ is constructed in advance, from the original image and its mean filtered image, using the formula:

$$\xi_k = \frac{1}{(1+\alpha)}\left[x_k + \frac{\alpha}{|N_k|}\sum_{x_r \in N_k} x_r \right] \quad , \tag{7}$$

where ξ_k - the gray value of the k^{th} pixel of the image ξ, x_r - the neighbors of x_k, N_k - the set of neighbors falling into a window around x_k and $\frac{1}{|N_k|}\sum x_r$ - the mean filter pixel value.

The fast clustering [19] is performed on the gray scale histogram of the newly created image ξ. In an analogous way, the objective function for fast segmenting is defined as

$$J_s = \sum_{i=1}^{C}\sum_{l=1}^{q} \gamma_l u_{il}^m (\xi_l - v_i)^2 \quad , \tag{8}$$

where v_i - center of the i^{th} cluster, u_{il} - fuzzy membership of gray scale value l in cluster i , q - number of the gray scale of the input image, which is generally much smaller than N, γ_l - number of the pixels having the gray value equal to l, where $l=1,\ldots, q$.

Thus, $$\sum_{l=1}^{q} \gamma_l = \mathrm{N} \tag{9}$$

For any value of l, under the conditions $\sum_{i=1}^{c} u_{il} = 1$, the objective function J_s is minimized by utilizing the Lagrangian multiplier method. The first derivatives of J_s with respect to u_{il} and v_i are obtained and equating them to zero. Then the two necessary conditions for J_s are obtained as follows:

$$u_{il} = \frac{(\xi_l - v_i)^{\frac{-2}{(m-1)}}}{\sum_{j=1}^{C}(\xi_l - v_j)^{\frac{-2}{(m-1)}}}, \text{ for } i = 1,2,\ldots,C \text{ and } l = 1,2,\ldots,q \tag{10}$$

and $$v_i = \frac{\sum_{l=1}^{q} \gamma_l u_{il}^m \xi_l}{\sum_{l=1}^{q} \gamma_l u_{il}^m} \text{ , for } i = 1,2,\ldots,C \tag{11}$$

The range of gray levels of the input image should be taken into account for the process time reduction; generally it is not considered in most of the FCM algorithms. That is why the gray value of the pixels is usually stored in 8 bits (in other words 256 levels in total). Thus the number of distinct gray levels q is generally considerably smaller than the size (N) of the image. As a resultant, in EnFCM the time complexity of clustering is reduced from O(NCI_1) to O(qCI_2).

3.2 Limitations of EnFCM

EnFCM is considerably faster than FCM_S algorithm and its variants. But the quality of the output cluster depends on (i) the size of the filter window, (ii) the value of the parameter α, and (iii) the filtering

method used.

3.3 Fast generalized fuzzy c-means algorithms (FGFCM)

When assigning a value to α, the following facts should be considered:

(1) The location (or spatial relationship) of pixels within the neighborhood window. For example, when the size of the filter window is extended from (3×3) to (5×5), α should be assigned to different value for different spatial distance from the center of the filter window, otherwise blurred output image would be the resultant,

(2) The gray scale relationship of the pixels within the same window will creep into the local neighborhood inhomogeneity of the window.

So assigning different values to α for different pixels within the window will suppress the influence of the outlier and avoid blur in the output image. To accelerate the process of clustering and at the same time choosing the value of α by an automated system according to the local (gray value and spatial distance) information [20] proposed a fast and robust FCM framework for image segmentation by using modified bilateral filter.

3.4 Bilateral filter

It is a non-linear denoising filter proposed by [21]. In denoising process of it, the gray scale value at each pixel in an image is replaced by an adaptive weighted average of gray values of neighbourhood pixels. This adaptive weight is calculated by a Gaussian distribution. The weights depend on Euclidean distance of pixels, and the radiometric differences of intensity. It preserves fine features of an image by systematically looping through each pixel and by adjusting the weights of the neighboring pixels accordingly. The mathematical formulation for bilateral filter is described below:

3.5 Mathematical model of bilateral filter

Let $X = \{x_{i,j}\}$, $(i = 1,2, \dots m,\ j = 1,2, \dots n)$ be the set of data points in the input image and $\xi = \{\xi_{i,j}\}$, $(i = 1,2, \dots m,\ j = 1,2, \dots n)$ be the output image processed. Here m and n represent the number of pixels does exist vertically and horizontally respectively.

Let the spatial similarity weightage for the pixel x_i (say) need to be calculated. A filter window of size $(1 + 2 * pad)$x$(1 + 2 * pad)$ is placed in such a way that x_i is the central pixel of the filter window, where *'pad'* is a positive integer.

The adaptive weightage S_{ij} has been introduced to incorporate both the local spatial weightage(S_{s_ij}) and the local gray level weightage(S_{g_ij}). Its multiplication model is given below:

$$S_{ij} = S_{s\_ij} \times S_{g\_ij} \quad (12)$$

where S_{s_ij} - local spatial similarity weightage, S_{g_ij} - local gray level similarity weightage, i^{th} pixel is the center of the local neighborhood filter window, andj^{th} pixels are the set of the neighbors falling into a local window around the i^{th} pixel.

The local spatial similarity weightage S_{S_ij} is given as follows:

$$S_{s\_ij} = exp\left(\frac{-\left([p_i-p_j]^2 + [q_i-q_j]^2 \right)}{\sigma_{s\_i}^2}\right), \quad (13)$$

where (p_i, q_i) - spatial coordinate of the central pixel x_i, (p_j, q_j) - spatial coordinate of $x_j \in N(x_i)$, and

$\sigma_{s\_i}^2$ – the scale factor of the spread of S_{s_ij} .

The local gray level similarity weightage S_{g_ij} is measured as

$$S_{g\_ij} = exp\left(\frac{-\|x_i-x_j\|^2}{\sigma_{g\_i}^2}\right), \quad (14)$$

where σ_{g_i} - a function of the local density around the central pixel x_i.

Its value represents the degree of gray scale smoothness in the local neighbourhood window. It is defined by

$$\sigma_{g\_i} = \sqrt{\frac{\sum\|x_j-x_i\|^2}{|N(x_i)|}}, \quad (15)$$

where x_i - the gray value of the central pixel within a special window, $x_j \in N(x_i)$,

$|N(x_i)|$- the cardinality of the neighbourhood pixels, and the summation runs over $N(x_i)$

By replacing the parameter α with S_{ij} , a new image ξ is generated as,

$$\xi_i = \frac{\sum_j s_{ij}x_j}{\sum_{j\in N_i} s_{ij}} \text{ , for } i = 1,2, \ldots N \text{ and } (x_j \in N(x_i)) \quad (16)$$

where ξ_i - the gray value of the i^{th} pixel of the new image ξ.

3.6 FGFCM

In [20], the value α of FGFCM was replaced with the adaptive weightage S_{ij} of bilateral filter (which is an automated system) to overcome the two limitations (mentioned in section 3.2) of using a common α. As

the pixels of an image are arranged in rectangular matrix form, to provide a rectangular filter with equal weightage to diagonal and non-diagonal neighbourhood pixels, in [20] the radial distance in numerator of equation (13) is modified as

$$S_{s\_ij} = exp\left(\frac{-max(\ |p_i - p_j|\ ,\ |q_i - q_j|\ )}{\lambda_s}\right)\ , \tag{17}$$

where λ_s – the scale factor of the spread of S_{s_ij} , and modified the equation (14) is of the form,

$$S_{g\_ij} = \ exp\left(\frac{-\|x_i - x_j\|^2}{\lambda_g \times \sigma_{g\_i}^2}\right), \tag{18}$$

where λ_g - the global scale factor of the spread of S_{g_ij} .

Finally the output image ξ is clustered by the equations (8) - (11).

3.7 Variants in FGFCM

(i) By assigning the value of S_{ij} in the equation (16) as

$$S_{ij} = \begin{cases} 1 & if\ j = i\ , \\ 0 & if\ j \neq i\ . \end{cases} \tag{19}$$

FGFCM algorithm is reduced into a fast version of the standard FCM.

(ii) By defining S_{ij} in (16) as

$$S_{ij} = \begin{cases} \frac{\alpha}{|N_j|} & if\ j \neq i\ , \\ 0 & if\ j = i\ . \end{cases} \tag{20}$$

FGFCM algorithm reduces into EnFCM.

(iii) By defining directly $S_{ij} = 1$ for all i and j in FGFCM framework, a variant FGFCM_S_1 was derived. (21)

(iv) Another variant FGFCM_S_2 was proposed by assigning the value of S_{ij} directly in the equation (16) as

$$S_{ij} = \begin{cases} 1 & if\ j = median\ of\ N(x_i)\ , \\ 0 & otherwise \end{cases} \tag{22}$$

When bilateral filter is used, the noise on the edges and in tiny areas of the input image creeps into the edges and tiny areas of output image [22, 23]. It influences more on the segmentation accuracy of FGFCM algorithm and its variants. This article proposes a mathematical model with bilateral filter and contrast limited adaptive histogram equalization (CLAHE) to overcome this problem.

4. Contrast limited adaptive histogram equalized fast fuzzy c-means clustering (AHFFCM)

4.1 Adaptive histogram equalization (AHE)

AHE is an image processing technique, used to improve the contrast of an image. Unlike the histogram equalization, it operates on tiles (a small data area). The contrast of each tile is enhanced, so that the specified histogram is well approximated. The AHE has an attitude of amplifying the noise in relatively homogeneous regions in the input image. A variant of AHE called contrast limited adaptive histogram equalization (CLAHE) suppresses it by limiting the amplification.

4.2 Contrast Limited Adaptive Histogram Equalization (CLAHE)

In CLAHE, the process of limiting the contrast is applied to each tile is proposed by [24]. Suppose any of the histogram bins have above the specified contrast limit. Then they are clipped and uniformly redistributed to other bins, before applying histogram equalization. After that, in order to eliminate artificially induced boundaries, the neighboring tiles are combined by bilinear interpolation. Figure (1) depicts the redistribution of the pixels in the clip limit $L_1 - L_2$.

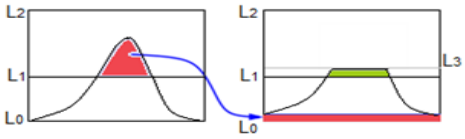

Figure (1): In CLAHE re-distribution of the pixels lying above the clip limit L_1L_2.

4.3 Bilinear interpolation

CLAHE is a time consuming process. By introducing interpolation, [24] improved the efficiency of contrast enhancement. In this method histogram, cumulative distribution function (CDF) and transformation function are calculated for each tile. The transformation functions are most suitable for the center pixel of the tiles. So the rest of the pixels are transformed with respect to the central pixels of the neighboring tiles. The pixels in the center part of the image (blue in color in figure (2)) are interpolated bilinearly. The pixels nearer to the boundary of the image (green in color) are interpolated linearly, and pixels close to the corners (red in color) are transformed with the transformation function of the corner tile. The coefficients of interpolation determine the position of the pixels among the center pixels of neighboring tile, so that the result is continuous as the pixel approaches a tile center and this procedure reduces the computation time.

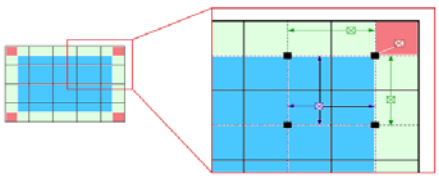

Figure (2): Illustration of bilinear interpolation.

4.4 Anisotropic diffusion

It is a technique proposed by [25] to denoise an image without removing fine features (like edges, lines) of input image. In this technique a family of parameterized images is generated. Here the resulting image is a combination of the original input image and a local adaptive filter image of the original image. In other words, anisotropic diffusion is a *space-variant non-linear* transformation of the input image. Here the space-variant filter is anisotropic. It depends on the content of the input image. The impulse noise near the edges and other structures is approximated in the output image, in different levels of the resulting scale space. In a generalized formulation, the local adaptive filter is replaced by a shape adaptive filter. The orientation along the structure stretches it accordingly.

4.5 Mathematical model for the proposed contrast limited AHFFCM algorithm

The input image is pre-processed, before the clustering as follows:

(i) The input image is denoised by the bilateral filter defined by the equations (16) – (18) and the new image ξ is constructed,
(ii) another new image *H* is constructed by applying CLAHE on the image ξ,
(iii) the output image *H* is smoothened further by anisotropic diffusion [26, 27], and
(iv) a new image A is constructed as a convex combination of the ξ and H, using the following equation

$$A = \{A_{ij} \mid A_{ij} = K * H_{ij} + (1-K)\xi_{ij}\},\ 0 < K < 1,\ \text{i= 1, 2 ...n, j=1, 2…m} \quad (23)$$

The number of tiles is a two-element vector of positive integers:$[Ro\ , Co]$ specifies the number of tile rows and tile columns. The total number of image tiles is equal to $(Ro * Co)$. It is calculated in such a way that each tile size is equal to the size of the neighbourhood window using the following equation:

$$Ro = \left\lfloor \frac{\text{No.of rows of input image}}{\text{size of Neighbourhood window}} \right\rfloor \quad \text{and}$$

$$Co = \left\lfloor \frac{\text{No.of Columns of input image}}{\text{size of Neighbourhood window}} \right\rfloor \quad (24)$$

where ⌊f⌋ denotes the integer part of f .

Note that in the proposed method the number of bins in CLAHE is fixed as (2*C-1).

4.6 Working rule for the proposed clustering method

Step 1. Initializing the following parameters:

(i) Number of clusters C.
(ii) Assign $\varepsilon > 0$ to a very small value.
(iii) Initialize prototype centers by random numbers.

Step 2. Calculate the local adaptive weightage S_{ij} by, using the equation (12) over the image.

Step 3. Construct a linearly-weighted summed image $\xi = \{\xi_1, \xi_2, \ldots, \xi_N\}$, here ξ_i is computed using the equation (16).

Step 4. Construct a new image *H* by applying CLAHE (with 2*C-1 bins) from ξ.

Step 5. Apply anisotropic diffusion on *H*.

Step 6. Construct a new image A, using the equation (23)

Step 7. Update the partition membership matrix $[u_{il}]$ using the equation (10).

Step 8. Update the cluster centers $\{v_1, v_2, \ldots, v_c\}$, using the equation (11).

Step 9. Repeat the steps 5 and 6, until the termination condition

$$|V_{old} - V_{new}| < \varepsilon \text{ is satisfied,}$$

where V_{old} and V_{new} are the set of prototype centers obtained in consecutive iterations.

5. Results and analysis

This section compares the performance of the AHFFCM with the existing six standard clustering algorithms FCM_S_1, FCM_S_2, FGFCM, EnFCM, FGFCM_S_1, and FGFCM_S_2 on synthetic, real and simulated MR images presented in [20]. In all these experiments the parameters are set as follows: $m = 2$, $\epsilon = 10^{-5}$. The algorithm is tested on the images corrupted by 'Gaussian', 'Salt and Pepper' and 'Mixed' noises separately. The results are evaluated by calculating its Segmentation Accuracy (SA) and Classification errors.

5.1 Segmentation Accuracy (SA)

It is calculated as [28, 29]

$$S_{ij} = \frac{A_{ij} \cap A_{ref\,j}}{A_{ij} \cup A_{ref\,j}}, \qquad (25)$$

where A_{ij} refers the set of pixels of the j^{th} cluster found by the i^{th} algorithm, and $A_{ref\,j}$ represents the set of pixels of the j^{th} cluster in the reference (original) segmented image.

5.2 Fixing the noise level and distribution, in mixed noise

When the mixed noise is used as a combination of the 'Gaussian' and "Symmetric α-Stable ($S\alpha S$)' noises, the combination of mixing the noises is given by the equation

$$P\eta = \eta S + (1-\eta)G,$$

where S - the Symmetric α -Stable noise, with location 0 and range γ_S, and

G - the Gaussian noise with mean zero and variance σ_G^2

Thus the characteristic function $\varphi(t)$ of $P\eta$ is formulated by [30] as,

$$\varphi(t) = exp\left(j\eta\theta t - (1-\eta)^2 \frac{\sigma_G}{2} t^2 - \eta^\alpha \gamma_S |t|^\alpha\right) \quad , \quad \eta \epsilon [0,1], \tag{26}$$

where α - the parameter, controlling the impulsive distribution as [30], $j = \frac{2}{(2+\pi)}$.

5.3 Results on synthetic image

The clustering efficiency of the above algorithms are compared by applying it, on a synthetic input image of size (128x128) pixels, with two classes of gray scale values 0 and 90. Three types of experiments are conducted on synthetic image.

5.3.1 Experiment 1

Here the image is corrupted at various levels in salt and pepper, Gaussian, and mixed noises separately. So, totally seven algorithms are applied on them. The parameters are fixed as $\lambda_g = 3$ (the optimal value obtained in [20], C=2, $|N_j|$=8 (a (3×3) neighbourhood window is placed on each pixel), K=0.25, clip limit =3x10^{-3}. At the same time in FCM_S_1, FCM_S_2 and EnFCM, the value of α is fixed at 3.8 (the optimal value obtained in [18].

Results on synthetic image corrupted with mixed noise

The clustering results on synthetic test image corrupted with mixed noise are presented in figure (3). The mixed noise used is as a combination of 'Gaussian white noise $N(0,100)$' and 'symmetric α-stable noise (α = 0.7)' with 0 mean and unit dispersion.

The clustering outputs are presented for visual comparison. Performances of FCM_S_1, FCM_S_2 and EnFCM are affected by the noise to different extents. It shows explicitly, that these algorithms are lacking behind in robustness to mixed noise. FGFCM_S_1 removes most of the noises. The proposed AHFFCM algorithm produces comparatively better output.

Quantitative comparison of the algorithms on synthetic image

The following table (1) compares the SA of the existing six algorithms with the proposed contrast limited AHFFCM on the synthetic images corrupted individually, by different noises, in different levels from 3% to 15%.

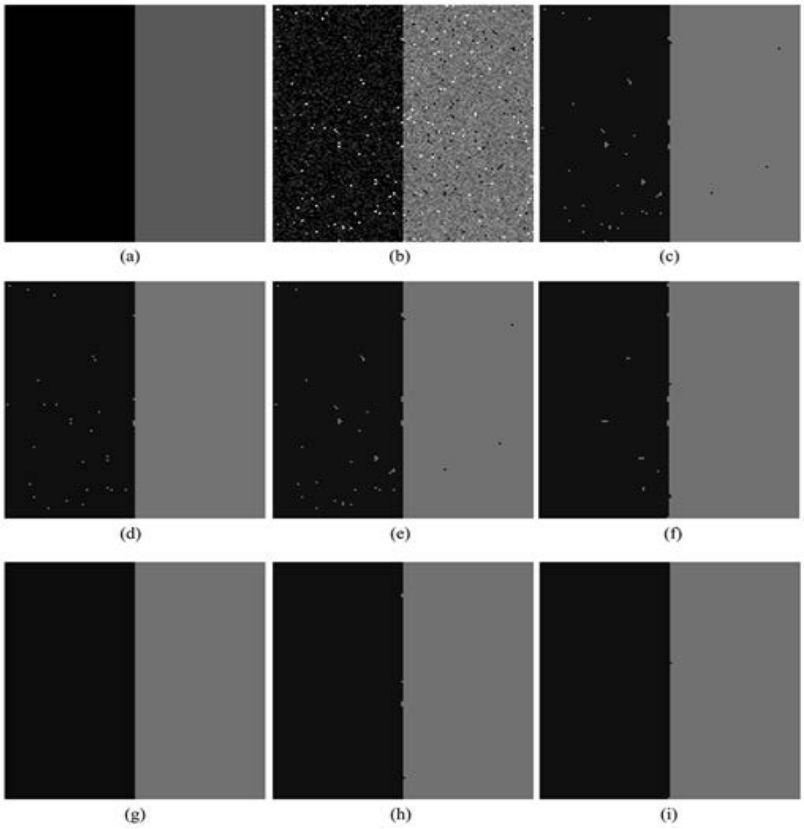

Figure 3: Cluster results on synthetic image. (a) Original image (b) The image with mixed noise. Result of (c) FCM_S_1 (d) FCM_S_2, (e) EnFCM, (f) FGFCM_S_1, (g) FGFCM_S_2, (h) FGFCM, (i) AHFFCM.

Table 1: SA % of seven algorithms on synthetic image

Noise Type	**Existing Algorithms**						**Proposed Algorithm**
	FCM_S1	**FCM_S2**	**EnFCM**	**FGFCM_S1**	**FGFCM_S2**	**FG_FCM**	**AHFFCM**
Gaussian 3%	98.65	98.20	98.74	98.71	97.86	98.70	**99.67**
Gaussian 5%	94.73	94.00	94.90	95.67	92.56	95.10	**98.98**
Gaussian8%	89.49	88.23	89.77	91.10	86.80	90.67	**98.61**
salt &pepper 5%	97.51	98.43	97.51	98.84	99.98	99.78	**99.99**
salt &pepper 10%	95.76	97.60	95.76	97.55	**100.00**	99.63	99.93
salt &pepper 15%	90.11	95.38	90.11	93.07	**99.91**	98.94	99.78
mixed noise α=0.3	93.80	97.24	95.34	95.81	99.65	97.75	**99.74**
mixed noise α=0.5	98.68	99.27	99.09	99.45	99.97	99.84	**99.98**
mixed noise α=0.7	99.38	99.62	99.40	99.69	**100.00**	99.91	99.93

- In presence of **Gaussian noise**, among the existing six algorithms, FGFCM_S_1 produces a better output. The proposed AHFFCM algorithm produces a better output than that of FGFCM_S_1.
- In the presence of **salt and pepper noise** among the existing six algorithms, FGFCM_S_2 produces a better output. AHFFCM algorithm produces comparable efficiency to FGFCM_S_2 in the presence of salt & pepper noise
- In presence of **mixed noise**, among the existing six algorithms, FGFCM_S_2 produces a better output. The proposed AHFFCM algorithm produces a better output than that of FGFCM_S_2 up to $\alpha = 0.5$.

From this results, it is observed that the AHFFCM algorithm relatively achieve a trade-off among the three types of noises. It is relatively suitable for clustering images when the image is corrupted by unknown or Gaussian or mixed noises.

5.3.2 Experiment 2

The crucial parameters in the clustering algorithms are noise dependent. So, it trivially influences the output. In the proposed AHFFCM and existing FGFCM algorithms λ_g is a crucial parameter, where as in FCM_S_1, FCM _S_2, and in EnFCM α is the crucial parameter. So, these parameters are suitably adjusted to improve the performance.

The objective of the experiment 2 on synthetic image is, to study the effect of various values of the crucial parameters λ_g and α in clustering efficiency. In this experiment, λ_g is assigned to the values 0 through 10 in steps of 1 where as α is assigned to the values 0 through 3 in steps of 0.25. The synthetic image in figure 3(a) is corrupted by three types of noises separately and the experiment is conducted on them. The graphical illustrations are in figure (4). It shows, that the variations of the number of misclassified pixels in FCM_S_1, FCM_S_2, EnFCM, and FGFCM, depends on the variation of the parameters λ_g and α. From figure 4(a) - 4(c), it is observed, that on all the three types of noises the misclassification of the proposed AHFFCM algorithm is almost independent of the choice of λ_g . Its performance is comparatively better than the existing algorithms.

5.3.3 Experiment 3

The objective of this experiment 3 on synthetic image is to study the effect of various values for the parameter *K* (in the equation (23)) in clustering efficiency. In this experiment *K* is assigned values 0 through 0.8 in steps of 0.1 in AHFFCM. The synthetic image in figure 3(a) is corrupted by three types of noises separately and the experiment is conducted on them. The results are presented graphically in figure 4(d). It reveals, that the variation of clustering efficiency in AHFFCM dependents on the variation of the parameter *K*, and the best performance is produced when *K*=0.25.

5.4 Results on real images corrupted by noises

5.4.1 Results on real image 'eight' with mixed noise using (3×3) neighborhood window

To test the clustering efficiency of the algorithm, it is applied on a real image '*eight*' [31] of size (308 x 242) contaminated simultaneously by Gaussian white noise N (0,180) with unit dispersion, zero mean and symmetric α stable ($S\alpha S$) noise with $\alpha = 0.9$, K= (1/No. of Bins), clip limit = $3x10^{-3}$. To compare the experimental results, the crucial parameters are set (as specified in [20] as: α=8 in FCM_S1, FCM_S2, En-FGM, and λ_g=2 in FGFCM and AHFFCM. For all the algorithms take C=3.

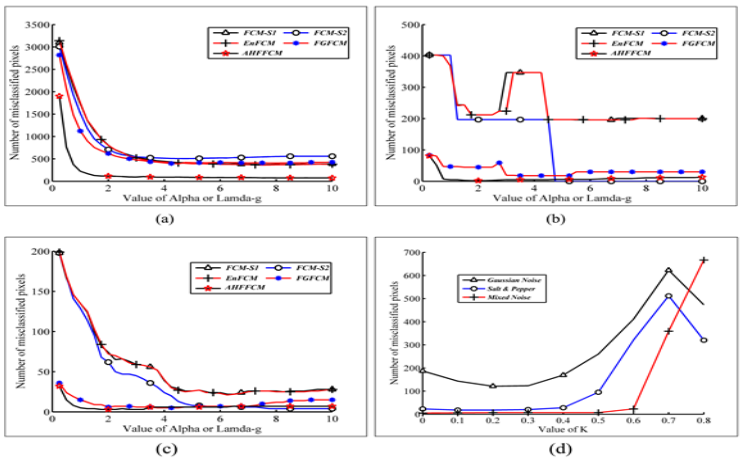

Figure 4: Classification errors against the parameters λ_g and α on the synthetic image corrupted separately with (a) Gaussian, (b) salt & pepper (c) mixed noise and (d) Classification errors against the parameter K.

The segmenting results of figure 5(b) are presented in figs.5(c) – 5(h) and the segmentation accuracy are compared in Table (2). From the results it is observed that all these algorithms are affected by the noise at different levels separately. The proposed algorithm performs better than that of the rest of the algorithms.

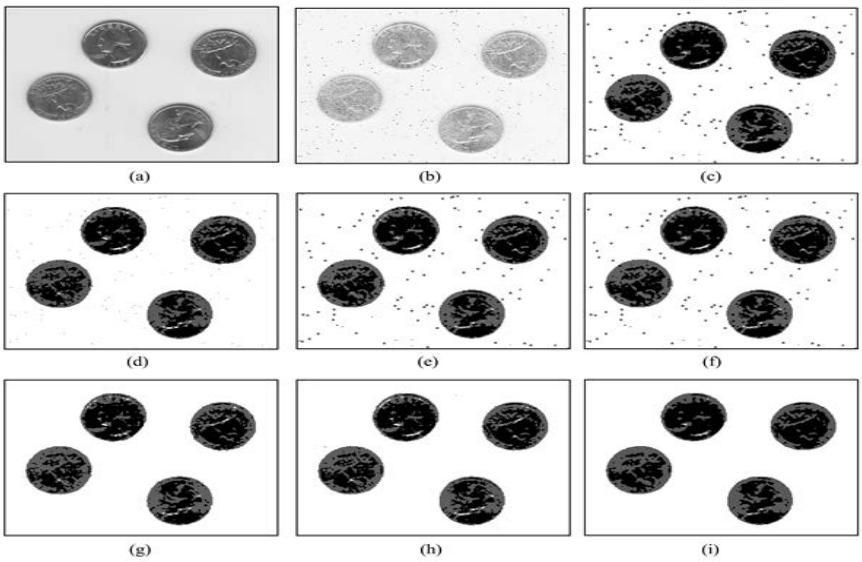

Figure 5: Segmentation results on real image '*eight*' corrupted with mixed noise. (a) Original image. (b) Noisy image. Outcomes by applying (c) FCM_S_1. (d) FCM_S_2. (e) EnFCM. (f) FGFCM_S_1. (g) FGFCM_S_2. (h) FGFCM (i) AHFFCM algorithms respectively.

In an analogous way, the AHFFCM algorithm is applied on the image '*eight*' corrupted separately by Gaussian noise and salt & pepper noise and compared with the results of the existing six algorithms.

5.5 Results using (5×5) neighborhood window on 'brain MRI', corrupted by mixed noise

For the comparative study of the proposed algorithm, a bigger size neighbourhood window on a real magnetic resonance image (MRI) of brain is chosen. The quantitative comparison of the existing six algorithms in [20] is used for the comparative study of the proposed algorithm.

To test the effect of using relatively bigger local window in the algorithm, it is applied on a brain MRI with a neighbourhood window of size (5×5) instead of the size (3×3). The real brain MRI of size (256 × 256) pixels, contaminated simultaneously by Gaussian white noise $N(0,180)$ with unit dispersion, zero mean and by symmetric α-stable ($S\alpha S$, $\alpha = 0.9$) noise. The clustered results of the seven algorithms are given in figure (6). To compare the results, the crucial parameters are set (as specified in [20] as $C = 3$, $\lambda_g = 0.5$, $\alpha = 5$ and $|N_j| = 24$, clip limit = 3 x 10^{-3}. K= (1/ No. of bins). From the results, it is observed, that when the window size is increased to (5×5), the output images of FCM_S_1, FCM_S_2, EnFCM, FGFCM_S_1 and FGFCM_S_2 are blurred heavily at different levels. But the blurring effect is reduced significantly, while applying FGFCM and AHFFCM algorithms. The less blurring area, while applying the proposed algorithm is encircled in figure 6(i). Thus, for a bigger neighbourhood window on real image, the clustering efficiency of AHFFCM algorithm is remarkable

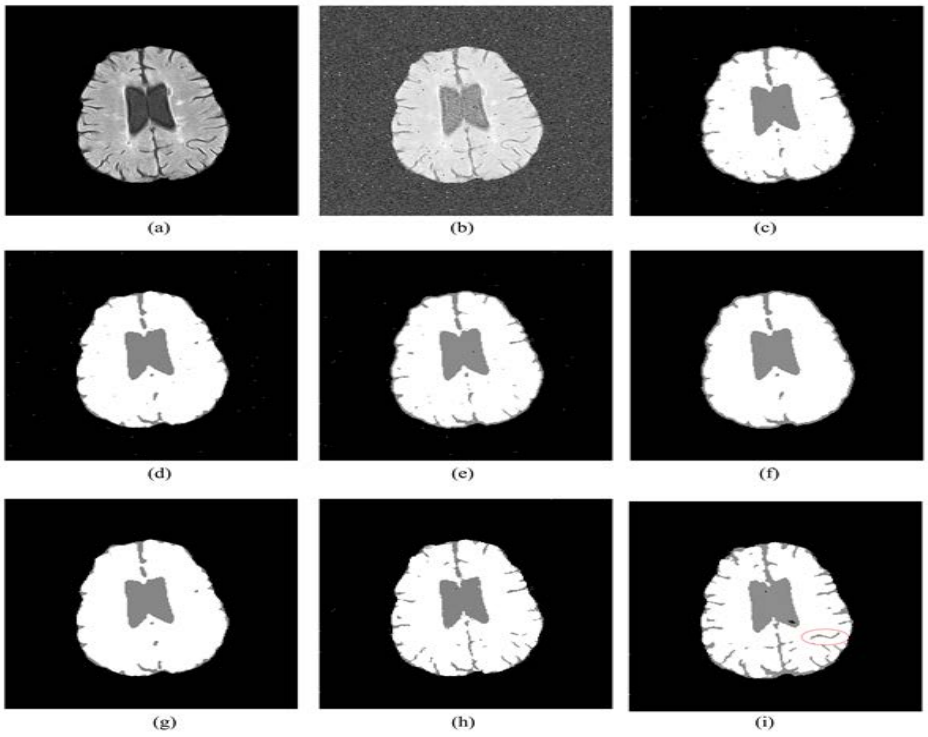

Figure 6: Clustering results obtained by using (5×5) neighborhood windows on a brain MRI: (a) Original image. (b) Corrupted image with mixed noise. Clustered results of (c) FCM_S_1, (d) FCM_S_2, (e) EnFCM, (f) FGFCM_S_1, (g) FGFCM_S_2, (h) FGFCM (i) AHFFCM

Table 2: Segmentation Accuracy (SA) of the seven algorithms corresponding to figs.(5) and (6)

		Cluster No.	Existing Algorithms						Proposed Algorithm
			FCM_S1	FCM_S2	EnFCM	FGFCM_S1	FGFCM_S2	FGFCM	AHFFCM
SA %	Figure 5(b-g)	1	67.41	66.00	67.53	67.52	63.96	71.26	**76.04**
		2	39.75	38.71	38.02	38.02	37.49	43.82	**61.04**
		3	97.66	97.89	96.98	96.98	98.02	98.30	**98.98**
	Figure 6(c-h)	1	99.58	99.88	99.59	99.40	99.85	99.88	**99.82**
		2	70.80	70.68	69.63	65.08	68.68	78.17	**88.66**
		3	92.53	92.28	92.15	91.10	91.85	94.37	**97.55**

5.6 Comparisons of processing time of clustering

In this section, the computational complexity of the seven algorithms, and experimental investigation of their practical acceleration for image clustering are analyzed. The fast and the standard segmentation methods of FCM are applied on the after-filtered images A_1 , A_2 , A_3 , A_4 and A_5. The images A_1 , A_2 , A_3 and A_4 are generated from the simulated brain MRI, given in fig 7(a). For that the equation (16) is employed, using the various algorithms of S_{ij} given in the equations (20) (21) (22) and (12). A_5 is generated using equation (24). Here the crucial parameters are set as C=8, α=0.8 in the equation (20) and λ_g=1 in the equation (12), respectively.

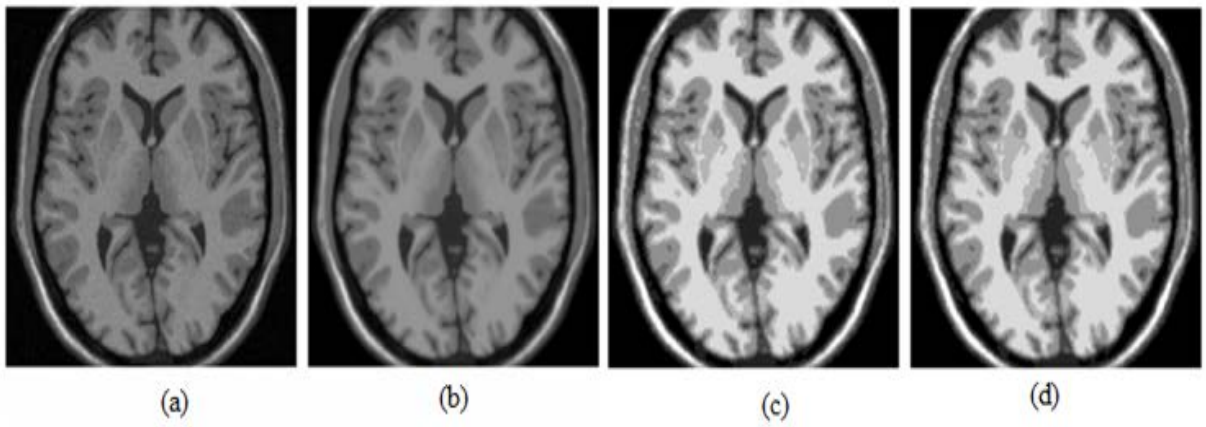

Figure 7: Segmentation results on simulated brain MRI. (a) Original T1-weighted image.

(b) The Filtered image A_5. (c) Using FCM for A_5 (d) Using fast FCM for A_5

The test image used is a T1-weighted [32] simulated MRI of 1 mm thickness with (181 x181) pixels. The noise level is set as 3% without any gray inhomogeneity. The sequence number of the slice in axial plane is 91. Segmentation process has been performed on the filtered image A_5 using FCM and fast FCM algorithms. The results are depicted in figure7(c) and 7(d) respectively. Similar results can be obtained by using both segmentation methods on the images A_1, A_2 , A_3 and A_4 respectively.

Table 3: Comparison of computational complexity between fast segmentation and FCM algorithms

Filter images	No. of Iteration		Running Time (in sec)	
	FCM	Fast FCM	FCM	Fast FCM
A_1	147	181	2.1553	0.1392
A_2	113	205	1.7642	0.1533
A_3	210	81	3.2209	0.0949
A_4	173	162	2.5429	0.1268
A_5	**212**	**58**	**3.1389**	**0.0631**

The computer used for segmentations has the following configurations: processor= Intel Core i5, CPU: 3.10 GHz, RAM = 4 G.B. Operating system: windows 7.0 (32 bit), Software: Matlab 11a. From Table (3), it is observed that the number of iterations of fast segmentation is fewer than FCM. The time taken for computation is drastically reduced due to the less number of gray levels (256) rather than the image size N (181 x181). When AHFFCM is used, the speed of clustering is comparatively higher than that of the existing methods. Moreover the segmentation accuracy is also higher than rest of the available methods.

6. Conclusion, scope and limitations

From the results presented, it is seen that AHFFCM performs comparatively better than FGFCM and other fast version of FCM algorithms. The results presented in this article reveal the fact, that the AHFFCM algorithm is appropriate. It is fast, insensitive to various types of noises and suitable for large-size gray images. Trilateral filter [33] can be used in denoising processes to preserve edges in color images in clustering.

Acknowledgement

The authors would like to thank Dr. Weiling Cai, Department of Computer Science & Engineering, Nanjing University of Aeronautics & Astronautics, Nanjing, P.R. China, for providing the test images used in their article [20].

References

[1] J.C. Bezdek, L.O.Hall, & L.P. Clarke, 'Review of MR image segmentation techniques using pattern recognition'. Medical Physics, vol. 20(4), pp. 1033-1048, 1993.

[2] W.M. Wells III, W.E.L. Grimson, R. Kikinis and F.A. Jolesz, "Adaptive segmentation of MRI data", IEEE Transactions on Medical Imaging, vol. 15, no. 4, pp. 429-442, 1996.

[3] M. S. Yang, Y. J. Hu, K. C. R. Lin and C. C. L. Lin, "Segmentation techniques for tissue differentiation in MRI of Ophthalmology using fuzzy clustering algorithms", Magnetic Resonance Imaging, vol. 20, no. 2, pp. 173-179, 2002.

[4] A. Ghosh, N. S. Mishra and S. Ghosh, "Fuzzy clustering algorithms for unsupervised change detection in remote sensing images", Information Sciences, vol. 181, no. 4, pp. 699-715, 2011.

[5] F. Höppner, Fuzzy cluster analysis: methods for classification, data analysis and image recognition. John Wiley & Sons, 1999.

[6] J. C. Bezdek, Pattern Recognition with Fuzzy Objective Function Algorithms. Springer Science & Business Media, 2013.

[7] G. C. Karmakar and L. S. Dooley, "A generic fuzzy rule based image segmentation algorithm", Pattern Recognition Letters, vol. 23, no. 10, pp. 1215-1227, 2002.

[8] J. K. Udupa and S. Samarasekera, "Fuzzy Connectedness and Object Definition: Theory, Algorithms, and Applications in Image Segmentation", Graphical Models and Image Processing, vol. 58, no. 3, pp. 246-261, 1996.

[9] S. M. Yamany, A. A. Farag and S. Y. Hsu, "A fuzzy hyperspectral classifier for automatic target recognition (ATR) systems", Pattern Recognition Letters, vol. 20, no. 11-13, pp. 1431-1438, 1999.

[10] D. L. Pham and J. L. Prince, "An adaptive fuzzy C-means algorithm for image segmentation in the presence of intensity inhomogeneities", Pattern Recognition Letters, vol. 20, no. 1, pp. 57-68, 1999.

[11] A. W. C. Liew, S. H. Leung and W. H. Lau, "Fuzzy image clustering incorporating spatial continuity", IEE Proceedings - Vision, Image, and Signal Processing, vol. 147, no. 2, p. 185, 2000.

[12] Y. A. Tolias and S. M. Panas, "Image segmentation by a fuzzy clustering algorithm using adaptive spatially constrained membership functions", IEEE Transactions on Systems, Man, and Cybernetics - Part A: Systems and Humans, vol. 28, no. 3, pp. 359-369, 1998.

[13] Y. A. Tolias and S. M. Panas, "On applying spatial constraints in fuzzy image clustering using a fuzzy rule-based system", IEEE Signal Processing Letters, vol. 5, no. 10, pp. 245-247, 1998.

[14] D. L. Pham, "Fuzzy clustering with spatial constraints", in IEEE Proc. Int. Conf. Image Processing, New York, 2002, pp. II-65–II-68.

[15] M. N. Ahmed, S. M. Yamany, A. A. Farag and T. Moriarty, "Bias field estimation and adaptive segmentation of MRI data using a modified fuzzy C-means algorithm", in IEEE Computer Society Conference, 1999, pp. [Vol. 1 pp. 250–255]. IEEE.

[16] M. N. Ahmed, S. M. Yamany, N. Mohamed, A. A. Farag, and T. Moriarty, “A modified fuzzy C-means algorithm for bias field estimation and segmentation of MRI data”, IEEE transactions on medical imaging, Vol.21, no.3, pp. 193-199, 2002.

[17] S. Chen and D. Zhang, "Robust Image Segmentation Using FCM With Spatial Constraints Based on New Kernel-Induced Distance Measure", IEEE Trans. Syst., Man, Cybern. B, vol. 34, no. 4, pp. 1907-1916, 2004.

[18] L. Szilagyi, Z. Benyo, S. M. Szilágyi and H. S. Adam, "MR brain image segmentation using an enhanced fuzzy c-means algorithm", in Proceedings of the 25th Annual International Conference of the IEEE, 2003, pp. Vol. 1, pp. 724-726, IEEE

[19] W. Cai, S. Chen and D. Zhang, "Fast and robust fuzzy c-means clustering algorithms incorporating local information for image segmentation", Pattern Recognition, vol. 40, no. 3, pp. 825-838, 2007.

[20] C. Tomasi and R. Manduchi, "Bilateral filtering for gray and color images", in Computer

Vision, 1998. Sixth International Conference, Bombay, pp. 839 - 846. IEEE,2008.

[21] F. Durand and J. Dorsey, “Fast bilateral filtering for the display of high-dynamic-range images”. in ACM transactions on graphics (TOG) (2002, July) , Vol. 21, No. 3, pp. 257-266, . ACM.

[22] S. Bae, S. Paris, and F. Durand, “Two-Scale Tone Management for Photographic Look,” In ACM Transactions on Graphics (TOG), 2006, Vol. 25, No. 3, pp. 637-645, ACM.

[23] K. Zuiderveld: Contrast Limited Adaptive Histogram Equalization. In: P. Heckbert: Graphics Gems IV, Academic Press 1994, ISBN 0-12-336155-9.

[24] P. Perona and J. Malik, "Scale-space and edge detection using anisotropic diffusion", IEEE Transactions on Pattern Analysis and Machine Intelligence, vol. 12, no. 7, pp. 629-639, 1990.

[25] J. Weickert. Anisotropic diffusion in image processing Stuttgart: Teubner, Vol. 1, pp. 59-60,1998

[26] P. Guidotti, "Some Anisotropic Diffusions", in Ulmer Seminare, 2009, pp. Vol. 14 , 215-221.

[27] C.T. Lin and C.G. Lee, “Real-time supervised structure/parameter learning for fuzzy neural network”. in Fuzzy Systems, 1992, IEEE International Conference on (pp. 1283-1291), IEEE.

[28] F. Masulli and A. Schenone, "A fuzzy clustering based segmentation system as support to diagnosis in medical imaging", Artificial Intelligence in Medicine, vol. 16, no. 2, pp. 129-147, 1999.

[29] A. Ben Hamza and H. Krim, "Image denoising: a nonlinear robust statistical approach", IEEE Transactions on Signal Processing, vol. 49, no. 12, pp. 3045-3054, 2001.

[30] http://Mathworks, Natick, MA. Image Processing Toolbox. [Online] Available: htttp://www.mathworks.com. [Accessed: May, 21- 2016]

[31] R. K. S. Kwan, A. C. Evans and G. B. Pike, "An Extensible MRI Simulator for Post-Processing Evaluation", in 4th International Conference on Visualization in Biomedical Computing, Springer-Verlag, 1996, pp. 135-140.

[32] P. Choudhury and J. Tumblin, “The trilateral filter for high contrast images and meshes”, In ACM SIGGRAPH (2005, July), Courses (p. 5). ACM.